*Journal of Applied Electrochemistry* **32**: 203–210, 2002.



# Surface characterization and photocatalytic reactivity of innovative $Ti/TiO_2$ and $Ti/Pt–TiO_2$ mesh photoelectrodes

X-Z. LI[1]* and F-B. LI[2]
[1]*Department of Civil and Structural Engineering, The Hong Kong Polytechnic University, Hunghom, Kowloon, Hong Kong*
[2]*Guangdong Key Laboratory of Agricultural Environment Pollution Integrated Control, Guangdong Institute of Eco-Environment and Soil Science, Leyiju, Guangzhou, 510650, Peoples Republic of China*
*(*author for correspondence, fax: +852 2334 6389; e-mail: cexzli@polyu.edu.hk)*

Received 8 January 2001; accepted in revised form 13 November 2001

*Key words:* mechanism, methyl orange, photoelectrocatalytic oxidation, platinum, titanium dioxide mesh

**Abstract**

Novel $Ti/TiO_2$ and $Ti/Pt–TiO_2$ mesh photoelectrodes were produced by anodizing titanium mesh in $H_2SO_4$ solution. Their structural and surface morphology were examined by X-ray diffraction (XRD), scanning electronic microscopy (SEM) and X-ray photoelectron spectroscopy (XPS). The analytical results indicated that the crystal structure, morphology and pore size were affected significantly by the voltage and current density applied in anodization and the percentage platinum content. The results of XPS measurement showed that the binding energy of O 1s and Ti 2p increased slightly owing to platinum deposition ($Pt^0$, $Pt^{2+}$ and $Pt^{4+}$) onto the $TiO_2$ surface. The photoelectrocatalytic (PEC) oxidation of methyl orange in aqueous solution using the $Ti/TiO_2$ and $Ti/Pt–TiO_2$ meshes was investigated. The experimental results demonstrated that $Ti/TiO_2$ mesh prepared at 160 V and 110 mA $cm^{-2}$ achieved the best PEC oxidation. The efficiency of PEC oxidation could be further enhanced by applying an electrical bias between the working electrode and counter electrode. An optimal electrical bias voltage was found to be 0.6 V, while an optimal platinum content was 3.37%.

## 1. Introduction

Although titanium dioxide ($TiO_2$) is an excellent photocatalyst and slurry-based photoreactors have been successfully employed for the decontamination of some natural systems and waste streams, $TiO_2$ solids recovery from decontaminated water is still a problem. The alternative of supported $TiO_2$ gives lower efficiency due to the loss of surface area and mass transfer limitations [1–3]. Fujishima and Honda in 1972 studied $TiO_2$ as a photoanode material and demonstrated its use for photooxidation of water, in which an electrical bias was applied between the anode and cathode, and the photogenerated electrons on $TiO_2$ were driven away from the anode in the process [4]. A number of studies demonstrated the higher efficiency of photoelectrocatalytic (PEC) oxidation processes for organic degradation, which can prevent carrier charge recombination and result in an extension of the lifetime of active holes [5–7]. In these studies, the photoanode was prepared by coating $TiO_2$ onto a conducting glass that was initially covered by an indium tinoxide. It was found that electron transfer between $TiO_2$ films and supporting carriers was not very efficient due to the poor connection between the two materials. Recently, we have successfully prepared an innovative $Ti/TiO_2$ mesh electrode by anodisation and used it for the PEC degradation of rose Bengal [8]. This mesh electrode had a large microporous surface area with excellent adsorption characteristics, which achieved a better PEC oxidation performance than using $TiO_2$ powder in suspension. To further improve its application in water and wastewater treatment, more detailed investigation is needed to determine the relationship between the preparation conditions and photoreactivity.

In this study the $Ti/TiO_2$-mesh electrodes were first prepared by anodization at different voltages and current densities, and the $Ti/Pt–TiO_2$ mesh electrodes were further prepared by photoreduction to deposit platinum on the surface of the $Ti/TiO_2$ mesh. The objectives of this research were: (i) to investigate the influence of voltage and current density during anodization on the crystal structure, surface morphology, chemical and electronic structure of the $Ti/TiO_2$-mesh electrode, and (ii) to seek optimal conditions to further enhance the PEC reactivity of $Ti/TiO_2$ mesh by surface modification.

## 2. Experimental details

### 2.1. *Materials*

Titanium mesh (purity 99.6%; nominal aperture 0.19 mm; wire dia. 0.23 mm; wires/inch $60 \times 60$; open area 20%, twill weave) was purchased from Goodfellow Cambridge Ltd. Methyl orange was purchased from Beijing Chemical Company. Other chemicals obtained were analytical grade and used without further purification. Deionized distilled water was used throughout the experiment.

### 2.2. *Preparation of $Ti/TiO_2$ mesh electrodes*

A large piece of raw titanium mesh with a thickness of 0.5 mm was cut into small rectangle pieces of 25 mm × 10 mm, which were then cleaned with alcohol and acetone solution, respectively. The pretreated titanium mesh and a copper plate of the same size were submerged in 0.5 M $H_2SO_4$ solution and an electrical current up to 200 V was applied using a laboratory-made d.c. power supply. In the first stage of anodization, galvanostatic anodization with a constant current (110 mA $cm^{-2}$) was applied with an increasing voltage at 1.2 V $s^{-1}$ within the first 2 min. In the second stage of anodization, a constant voltage (80, 120, 140, 160, 180 and 200 V) was then maintained, while the current density was gradually decreased from 110 to 33 mA $cm^{-2}$. The whole anodization process lasted for about 10 min. The $Ti/TiO_2$ mesh electrodes prepared at the different electrical voltages were named 80, 120, 140, 160, 180 and 200 V-mesh, respectively. Also, more electrodes were prepared with different current densities (80, 110, 140 and 170 mA $cm^{-2}$) in the first stage; only 160 V was used in the second stage. These were correspondingly named 80, 110, 140 and 170 mA-mesh. The freshly generated $TiO_2$-mesh electrodes were rinsed with 0.001 M nitrate acid and distilled water, then dried in an oven at 105 °C for 2 h.

### 2.3. *Preparation of $Ti/Pt–TiO_2$ mesh electrode*

The anodized $Ti/TiO_2$ mesh electrodes were further modified by photoreduction to deposit platinum onto the $TiO_2$ layer. In this method the $Ti/TiO_2$ mesh was placed in the 0.1 M methanol solution containing a certain amount of hexachloroplatinic acid as a hole scavenger. The solution was irradiated with a 125 W high-pressure mercury lamp for 20, 40, 60 and 80 min respectively. The product electrode was washed repeatedly with water and dried at 105 °C for 2 h. The platinum content on the mesh surface was detected by X-ray photoelectron spectroscopy (XPS). Four pieces of electrode prepared had platinum contents of 1.58%, 3.37%, 6.69% and 11.13% (mol $mol^{-1}$) and were correspondingly labelled as Pt1-mesh Pt2-mesh, Pt3-mesh and Pt4-mesh.

### 2.4. *Characterization of $Ti/TiO_2$-mesh electrode*

To determine the crystal phase composition of the $Ti/TiO_2$ mesh electrodes, X-ray diffraction (XRD) measurement was performed at room temperature with a Philips PW3710 diffractometer using Cu$K_\alpha$ radiation ($\lambda_a = 0.154\,060$ nm; $\lambda_0 = 0.154\,439$ nm); accelerating voltage was 40 kV, and emission current was 30 mA. Scanning electron microscopy (SEM) (Leica Stereoscan, 400i series) was used to study surface morphology, average pore size and pore distribution. High tension was selected at 15 kV. To determine the crystal phase composition of the mesh, X-ray photoelectron spectroscopy (XPS) was recorded with a PHI Quantum ESCA microprobe system, using the Mg$K_\alpha$ line of a 250 W Mg X-ray tube as a radiation source with the energy of 1253.6 eV, 16 mA × 112.5 kV. A working pressure of $12 \times 10^{-8}$ N $m^{-2}$ was applied. As an internal reference for the absolute binding energies, the C 1s peak of hydrocarbon contamination was used. The fitting XPS curves were analysed using Multipak 6.0A.

### 2.5. *Equipment*

The experiment of PEC oxidation was performed in a batch photoreactor, which consisted of a cylindrical borosilicate glass vessel with an effective volume of 165 ml, a 125 W high-pressure mercury lamp (Institute of Electric Light Source, Beijing), a potentiostat (ISO-TECH 1PS 1810H), a mesh electrode as anode and a Cu plate electrode (50 mm × 10 mm) as cathode. The high-pressure mercury lamp was positioned inside the vessel surrounded by a circulating water jacket (Pyrex). The two electrodes were positioned in parallel and connected with a potentiostat. In the experiment, the methyl orange solution was gently aerated under u.v. irradia-

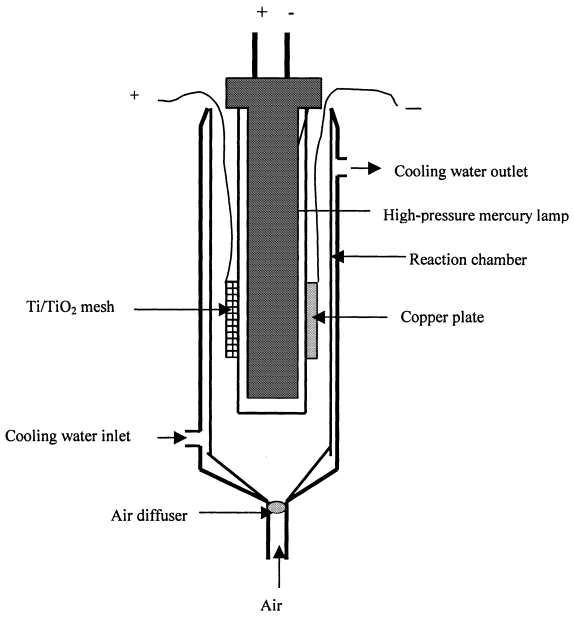


*Fig. 1.* Photoreactor system.

tion and samples were collected at different times for analyses.

### 2.6. *PEC oxidation of methyl orange in aqueous solution*

Four sets of tests were carried out with different objectives. The first set was carried out using the Ti/$TiO_2$ electrodes made at constant current density (110 mA) but different working potentials (80, 120, 140, 160, 180 and 200 V) under the same light intensity for 85 min to determine the optimal voltage applied in the anodising process. The second set was conducted using the Ti/$TiO_2$ electrodes prepared with the same voltage (160 V), but different working current densities (80, 110, 140 and 170 mA $cm^{-2}$) to determine the optimal current density. The third set was performed using the Ti/Pt–$TiO_2$ electrodes with different platinum content to study the optimal ratio between platinum and $TiO_2$ on the mesh. The fourth set was conducted by applying different electrical potentials between the working electrode and counter electrode to determine the optimal voltage for the reaction.

### 2.7. *Analytical methods*

The methyl orange concentration in aqueous solution was determined by u.v.–vis. spectroscopy (Genesys-2) at maximum absorption wavelength and total organic carbon (TOC) was monitored with a TOC analyser (Shimadzu 5000A) equipped with an autosampler (ASI-5000). The light intensity was measured by a Black-ray u.v. (UVP Inc, model J 221).

## 3. Results and discussion

### 3.1. *Crystal structure*

The crystal phase composition of the Ti/$TiO_2$-mesh electrodes prepared with different voltages and current densities was examined by XRD. The diffractograms Ti/$TiO_2$ meshes are shown in Figure 2(a) and (b), respectively, where the peaks representing anatase and rutile are correspondingly labelled as A and R. For the 80 V-mesh, 120 V-mesh and 140 V-mesh, it was found that

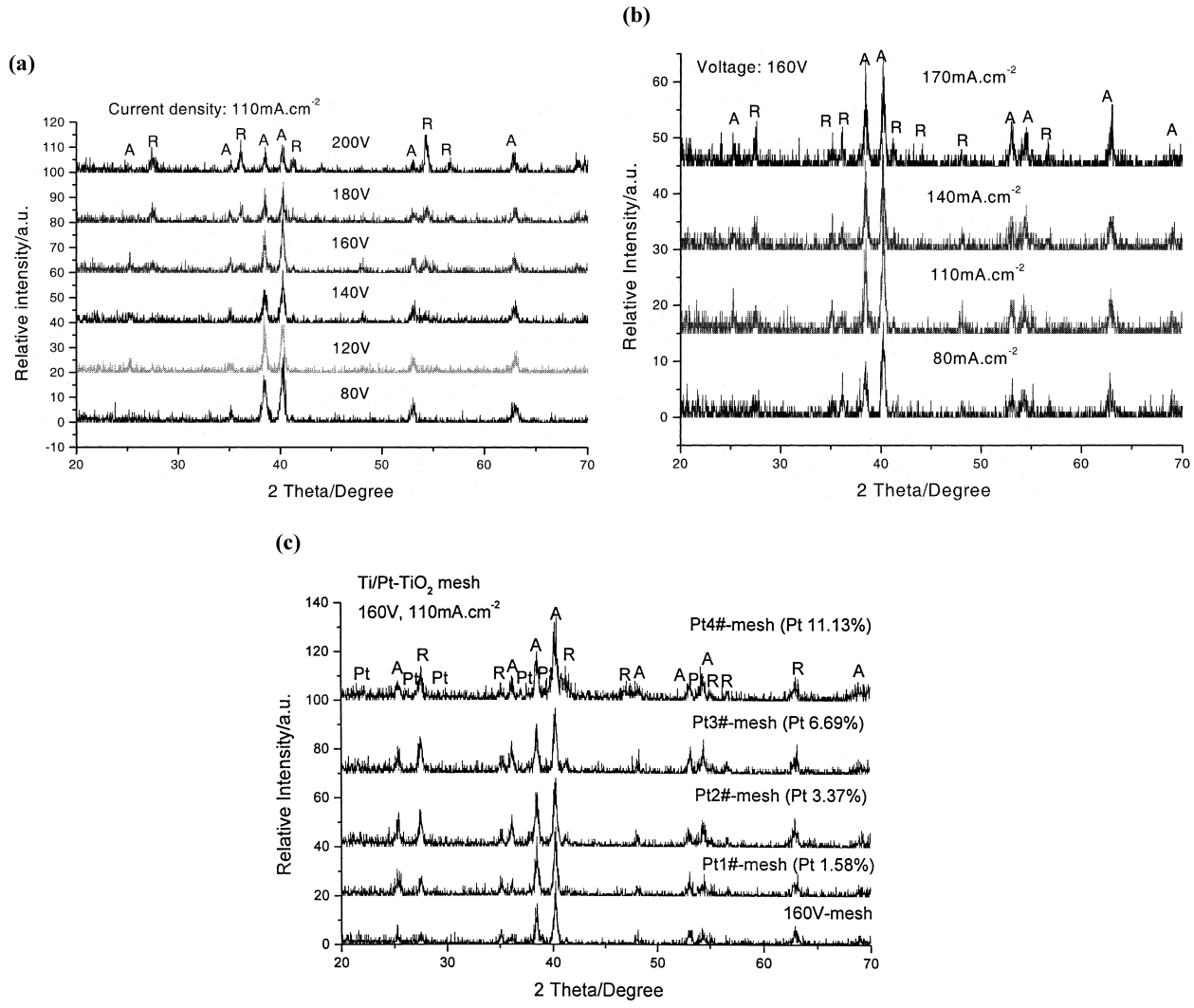


*Fig. 2.* X-ray diffraction of the Ti/$TiO_2$ electrodes: (a) prepared at different voltages (A anatase; R rutile); (b) prepared at different current densities; and (c) with different platinum content.

only anatase phase presented. When the anodization voltage went up to 160 V, rutile phase turned up at 27.405 (1 1 0), 36.105, 41.310 and 56.685, respectively. The intensity of rutile peaks increased with increase in anodization voltage. Even though the anodization voltage further increased to 200 V, the 1 0 1 peak of anatase phase was very weak, and the intensity of all other anatase peaks decreased, whereas rutile peaks increased. When the anodization voltage was fixed at 160 V and the current density varied from 80 to 170 mA $cm^{-2}$, all the peaks of anatase and rutile increased with increase of current density. The diffractograms of Ti/Pt–$TiO_2$ meshes are shown in Figure 2(c). It can be seen that the intensity of anatase and rutile peaks increased with the increase of platinum content. For all the Ti/Pt–$TiO_2$ meshes, 1 0 1 peak and 1 1 0 peak presented significantly, compared to that of Ti/$TiO_2$ mesh (160 V-mesh). For the Pt4-mesh, some Pt peaks presented.

### 3.2. *Surface morphology and pore distribution*

The surface morphology of the Ti/$TiO_2$-mesh electrodes was examined by SEM and the analytical results of the meshes made at different voltages and current densities are shown in Figure 3. It was found that the surface of the oxidized meshes had a microporous structure and was rougher than that of the raw Ti mesh. The results demonstrated that the $TiO_2$ film formed on the mesh at a higher voltage in the anodization was thicker. The pore size of the oxidized meshes varied from 10 to 120 nm, as the applied anodizing voltage increased from 80 to 200 V. In the meantime, the pore size grew fast when the voltage increased from 80 to 160 V, and grew slowly when the voltage exceeded 160 V. The earlier work [9] on the titanium anodization indicated that the formation of micropores was attributed to power dissipation in the barrier oxide layer. When anodizing current density is greater than 30 mA $cm^{-2}$ in sulfuric acid, the power dissipated in the barrier oxide layer increases considerably. It causes overheating of local oxide, and cooling of the oxidized anode by the electrolyte becomes insufficient. The higher temperature leads to a higher ionic current, probably along grain boundaries, and the oxide may recrystalize and result in a porous surface. With current densities greater than 100 mA $cm^{-2}$, a fast dissolution of the oxide is believed to occur with the creation of pores, leading to an even rougher surface.

In this study, the surface morphology of the Ti/Pt–$TiO_2$ meshes also appeared different owing to the platinum deposition on the surface as shown in Figure 4. When the mesh contained 1.58% of platinum (Pt1-mesh), the platinum clusters were formed with a size of 15–30 nm and only a small portion of the $TiO_2$ surface was covered. However, when the mesh contained platinum up to 11.13% (Pt4-mesh), the size of clusters increased significantly from 15 to 70 nm and the platinum deposit filled up most pores on the $TiO_2$ surface.

### 3.3. *Chemical and electronic structure*

To determine the chemical and electronic structure of the mesh surface and also the valence states of various species, five meshes of 160 V-mesh (no Pt), Pt1, Pt2, Pt3 and Pt4 were examined by XPS and the XPS spectra of O 1s, Ti 2p and Pt 4f are shown in Figure 5. The specifications of Ti 2p, O 1s and Pt 4f for the different

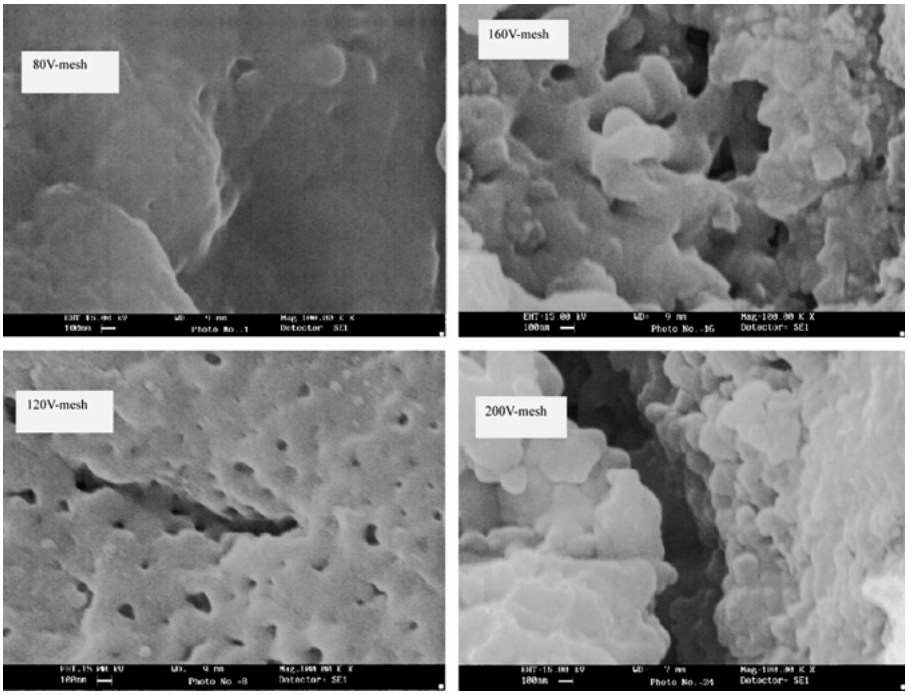


*Fig. 3.* Micrographs of Ti/$TiO_2$ meshes prepared at 110 mA, but different voltages.

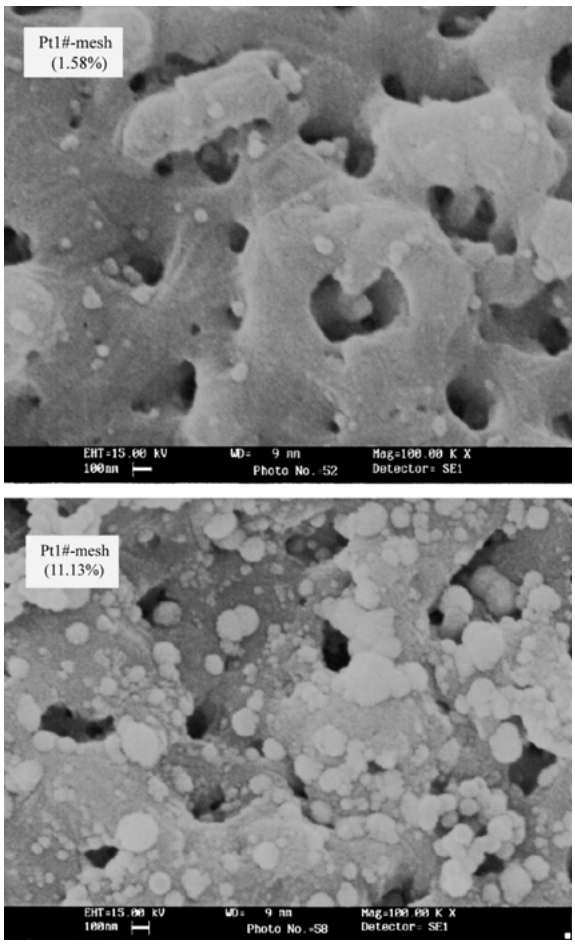


*Fig. 4.* Micrographs of $Ti/TiO_2$ mesh with different platinum content.

meshes were obtained and are listed in Tables 1 and 2. The results in Figure 5(a) and Table 1 demonstrated that the O 1s curves had a two-band structure. The main O 1s peak between 529.68–530.31 eV increased with increase in platinum content. Another O 1s peak at 531.78–531.85 eV may be attributed to $Pt(OH)_2$ or $PtO_2$. Significantly, the relative area of the O 1s band attributed to $TiO_2$ decreased with increase in platinum content, since the platinum cluster covered the surface of the $Ti/TiO_2$ mesh.

The results in Figure 5(b) showed that the Ti 2p peaks of the $Ti/Pt–TiO_2$ meshes were narrow with slight asymmetry and decreased significantly with increase in platinum content. Meanwhile, the data in Table 1 indicated that the Ti 2p had a binding energy in the range 458.35–458.74 eV, attributed to $Ti^{4+}$ which increased slightly with the increase in platinum content. The Pt 4f spectra shown in Figure 5(c) demonstrated that the $Ti/Pt–TiO_2$ meshes consisted of four peaks, corresponding to $Pt^0$, $Pt^{2+}$ and $Pt^{4+}$, respectively. The data in Table 2 indicated that the peaks at 70.67–71.40 eV were attributable to metallic platinum as $Pt^0$; the peaks at 71.96–72.69 eV were peculiar to either $Pt(OH)_2$ or $PtCl_4^{2-}$ as $Pt^{2+}$; the peaks at 74.48–75.07 eV to $PtO_2$ as $Pt^{4+}$ and the peaks at 77.53–78.40 eV to $PtCl_6^{2-}$ also as $Pt^{4+}$. In this photoreduction process,

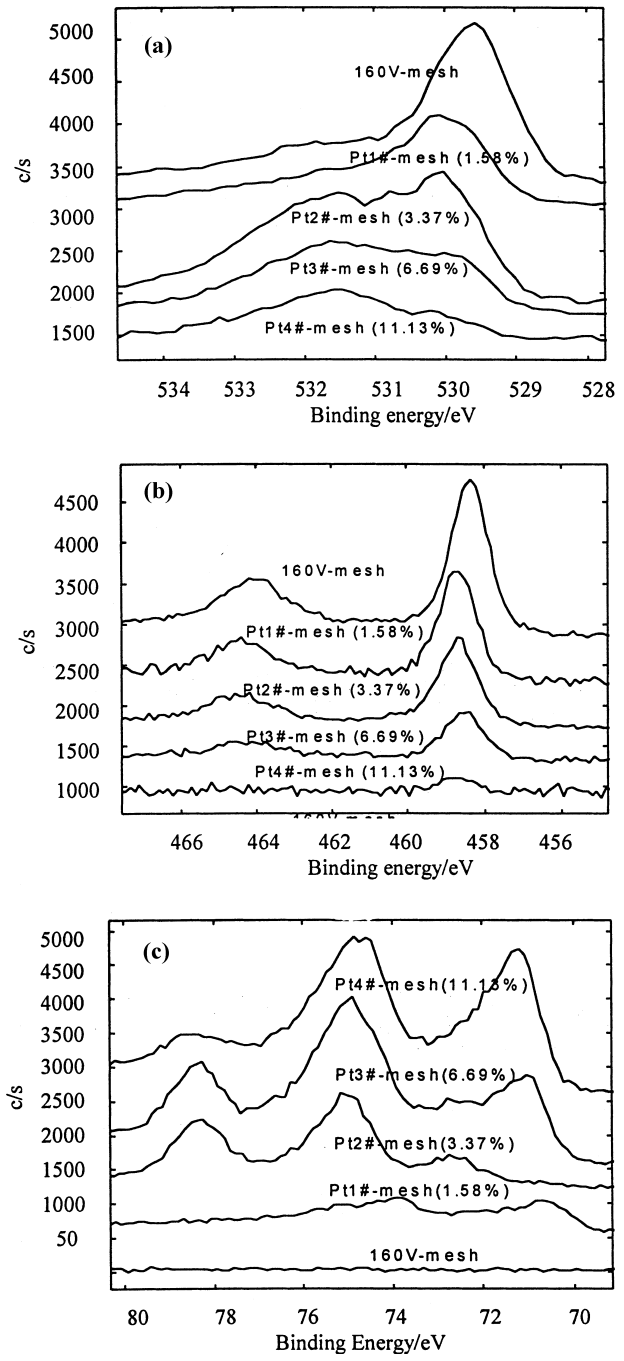


*Fig. 5.* Spectra of O 1s (a), Ti 2p (b) Pt 4f and (c) states in the XPS analysis.

$PtCl_6^{2-}(Pt^{4+})$ was adsorbed on the surface of the $Ti/TiO_2$ mesh first, and then reduced into $PtCl_4^{2-}$ $(Pt^{2+})$ and further to metallic platinum $(Pt^0)$. However, the photoreduction of $PtCl_6^{2-}$ was incomplete and therefore a certain amount of $Pt^{4+}$ still remained on the $Ti/Pt–TiO_2$ meshes.

### 3.4. *PEC oxidation of methyl orange*

The first set of tests was carried out using $Ti/TiO_2$ meshes anodized at the same current density of 110 mA $cm^{-2}$ but at different voltages of 80, 120, 140,

*Table 1.* Data of O 1s and Ti 2p in XPS analysis

| Catalysts | Ti 2p | O 1s (1/2) | | | O 1s (2/2) | | |
|---|---|---|---|---|---|---|---|
| | | BE /eV | FWHM /eV | Area /% | BE /eV | FWHM /eV | Area /% |
| $TiO_2$ | 458.41 | 529.68 | 1.43 | 100 | | | |
| Pt1 | 458.50 | 530.19 | 2.22 | 75.16 | 531.85 | 0.92 | 24.84 |
| Pt2 | 258.65 | 530.01 | 1.38 | 70.27 | 531.79 | 1.48 | 29.73 |
| Pt3 | 458.74 | 530.09 | 1.47 | 47.14 | 531.87 | 1.58 | 52.86 |
| Pt4 | 458.70 | 530.31 | 1.45 | 23.90 | 531.78 | 1.66 | 76.10 |

*Table 2.* Data of Pt 4f, valence state, platinum content (%) obtained from the fitted curve

| Catalysts | Pt /% | $PtCl_6^{2-}$ | | | $PtO_2$ | | | $Pt^{2+}$ | | | $Pt^0$ | | |
|---|---|---|---|---|---|---|---|---|---|---|---|---|---|
| | | BE /eV | FWHM /eV | Area /% | BE /eV | FWHM /eV | Area /% | BE /eV | FWHM /eV | Area /% | BE /eV | FWHM /eV | Area /% |
| Pt1 | 1.58 | 78.40 | 1.20 | 23.90 | 75.07 | 1.59 | 52.98 | 72.65 | 1.74 | 20.30 | 70.71 | 1.41 | 2.82 |
| Pt2 | 3.37 | 77.53 | 3.20 | 27.94 | 74.48 | 2.53 | 45.17 | 71.96 | 2.20 | 17.59 | 70.85 | 1.05 | 9.30 |
| Pt3 | 6.69 | 77.97 | 2.22 | 18.26 | 74.67 | 2.20 | 45.18 | 72.02 | 2.20 | 19.32 | 70.67 | 0.71 | 17.25 |
| Pt4 | 11.13 | 78.06 | 3.20 | 17.40 | 74.84 | 2.20 | 47.86 | 72.69 | 2.20 | 7.83 | 71.40 | 1.15 | 26.90 |

(BE: binding energy; FWHM: full width at a half of the maximum height of peaks).

160, 180 and 200 V, respectively, to photodegrade methyl orange (MO) in aqueous solution under a light intensity of 4.38 mW $cm^{-2}$, but without applying any electrical bias. Six tests were performed with an initial MO concentration of 10 mg $l^{-1}$ and samples were collected at different reaction times (0, 10, 25, 40, 55, 70 and 85 min) for analysis of u.v.–vis. absorption. The first-order kinetic constant $k$ in each test was calculated based on the experimental data of methyl orange removal as shown in Figure 6. The experiment demonstrated that the $Ti/TiO_2$ electrode anodized at 160 V achieved the best photocatalytic reactivity, the reaction rate in this PEC oxidation using the 160 V-mesh was three times higher than that using the 80 V-mesh, and was almost double that using the 200 V-mesh.

The second set of tests was carried out by applying the $Ti/TiO_2$ mesh anodized at the same voltage of 160 V but at different current densities of 80, 110, 140 and 170 mA $cm^{-2}$. Other conditions were the same as those in the first set of tests. The removal of methyl orange demonstrated that the 110 mA-mesh had the best photocatalytic reactivity, since the first-order kinetic constant $k$ using the 110 mA-mesh was almost double that using the 80 and 170 mA-mesh, as shown in Figure 7. The results in these two sets of tests indicated that the optimal conditions in the anodization process to prepare a $Ti/TiO_2$ mesh with the best PEC reactivity should be set at 160 V and 110 mA $cm^{-2}$.

To investigate the effect of platinum content on the photocatalytic reactivity, the third set of tests was conducted using the 160 V-mesh (0%), Pt1-mesh (l.58%), Pt2-mesh (3.37%), Pt3-mesh (6.69%) and Pt4-mesh (l1.13%) under light intensity of 4.38 mW $cm^{-2}$, but without applying electrical bias. Methyl orange solutions with the initial concentration of 10 mg $l^{-1}$ were irradiated for 85 min and the results are shown in

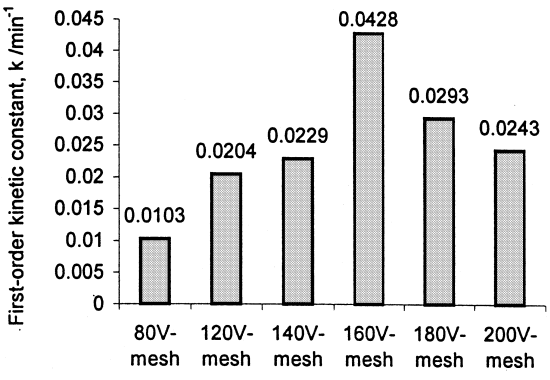


*Fig. 6.* Rates of the methyl orange photodegradation using the $Ti/TiO_2$ electrodes prepared at different voltages.

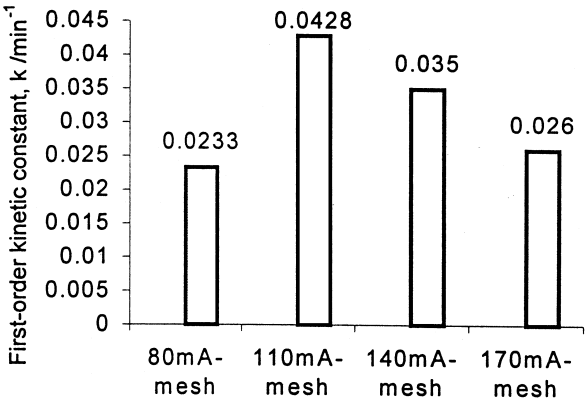


*Fig. 7.* Rates of methyl orange photodegradation using the $Ti/TiO_2$ electrodes prepared at different current densities.

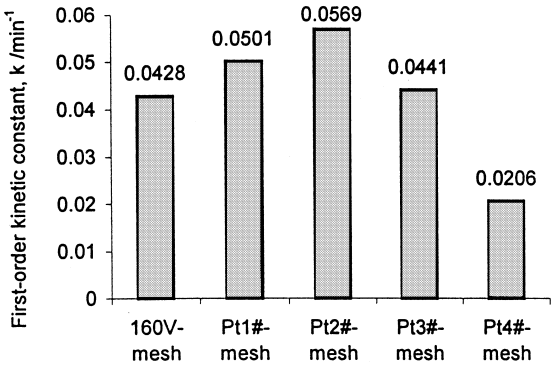


*Fig. 8.* Rates of methyl orange photodegradation using different $Ti/Pt-TiO_2$ electrodes.

Figure 8. The results demonstrated that the photocatalytic oxidation of methyl orange was significantly affected by the platinum content contained in the meshes from 1.58 to 11.13%. It seemed that there was an optimal platinum content of around 3.37% to achieve the highest photocatalytic reactivity.

The fourth set of tests was carried out using the 160 V-mesh with the same light intensity and the same initial methyl orange concentration, but applying different electrical bias (0.0, 0.1, 0.3, 0.6 and 1.0 V) between the two electrodes. One test was also carried out as PC oxidation, in which the $Ti/TiO_2$ electrode and counter electrode were not electrically connected. All tests lasted for 85 min and the experimental results are shown in Figure 9. The experiment demonstrated that 0.6 V was the best voltage for application of the electrical bias, although the first-order kinetic constant $k$ had only a slight increase in the range of 0.0–1.0 V. We found there was a significant difference between PC and PEC oxidation, which means that whether the two electrodes were connected was more important than the voltage variation between the two electrodes for the reaction rate.

To investigate the mineralisation of methyl orange, TOC in methyl orange solutions was also monitored in the reactions using the 160 V-mesh and Pt2-mesh electrodes, respectively, with a light intensity of 4.38 mW $cm^{-2}$ and 0.6 V bias. Samples were collected at 0, 20, 40, 60, 80, 100 and 120 min for TOC analysis. The results shown in Figure 10 show that the TOC was removed by

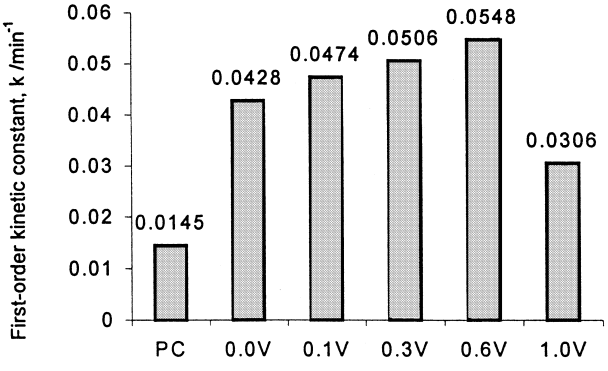


*Fig. 9.* Rates of methyl orange photodegradation by applying different electrical bias.

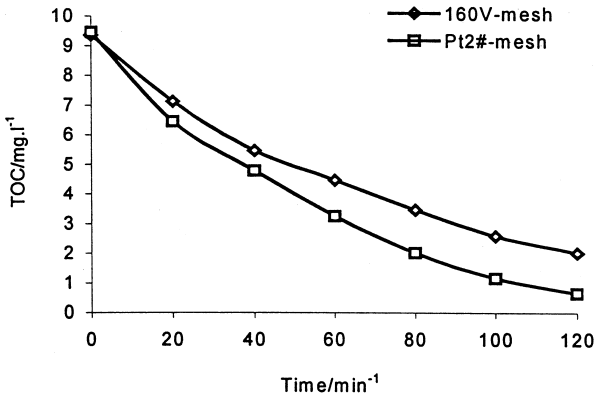


*Fig. 10.* TOC removals using the 160 V-mesh and Pt2-mesh by applying 0.6 V bias.

78.5% and 93.1%, respectively, when 160 V-mesh and Pt2-mesh were used. This confirmed that the $TiO_2$ mesh electrode with platinum impurity (Pt2-mesh) had a better PEC reactivity than the mesh with $TiO_2$ only (160 V-mesh) in the mineralization of methyl orange. The experiment demonstrated that a complete mineralization of methyl orange could be achieved within 120 min under this experimental condition.

### 3.5. *Mechanism of PEC oxidation using $Ti/TiO_2$ and $Ti/Pt–TiO_2$ mesh electrodes*

We propose that the mechanism of PEC oxidation using a $Ti/TiO_2$ working electrode and a copper counter electrode can be expressed by Equations l–7:
Working electrode (WE)

$$Ti/TiO_2 \Rightarrow ((Ti/TiO_2)-e_{cb})_{WE} + ((Ti/TiO_2)-h^+_{vb})_{WE} \quad (1)$$

$$((Ti/TiO_2)-e_{cb})_{WE} \Rightarrow (Cu-e)_{CE} \quad (2)$$

Counter electrode (CE)

$$2\,(Cu-e)_{CE} + 2\,H_2O \Rightarrow H_2 + 2\,OH \quad (3)$$

where the subscripts 'cb' and 'vb' denote the conduction and valence bands of the $TiO_2$, respectively.
Overall reaction

$$Ti/TiO_2 + H_2O \Rightarrow \frac{1}{2}\,H_2 + OH + ((Ti/TiO_2) - h^+_{vb})_{WE} \quad (4)$$

The holes on the WE react with the hydroxide or $H_2O$ molecules adsorbed on the $TiO_2$ surface ($OH_s$ and $H_2O_s$) to generate hydroxyl radicals (OH·):

$$OH^-_s + ((Ti/TiO_2-h^+_{vb})_{WE} \Rightarrow (Ti/TiO_2)_{WE}-OH\bullet \quad (5)$$

$$H_2O_s + ((Ti/TiO_2)-h^+_{vb})_{WE} \Rightarrow (Ti/TiO_2)_{WE}-OH\bullet + H^+ \quad (6)$$

Finally the hydroxyl radicals (OH•) oxidize the methyl orange adsorbed on the WE surface.

$$(\mathrm{Ti/TiO_2})_{\mathrm{WE}} - \mathrm{OH}\bullet + \text{methyl orange} \Rightarrow \cdots \cdots \Rightarrow \mathrm{CO_2} + \text{inorganic ions} + (\mathrm{Ti/TiO_2})_{\mathrm{WE}} - \mathrm{H_2O_s} \quad (7)$$

When the Ti/Pt–$TiO_2$ mesh is used, the excited electrons from valence band to conduction band migrate to platinum clusters, and then further migrate to $O_2$ molecules adsorbed on the mesh surface to form $O_2^-$. The $O_2^-$ is an active species to oxidize methyl orange as shown in Equations 8–10.

$$\mathrm{Ti/Pt–TiO_2} \Rightarrow ((\mathrm{Ti/Pt–TiO_2}) - \mathrm{e_{cb}})_{\mathrm{WE}} + ((\mathrm{Ti/Pt-TiO_2}) - \mathrm{h^+_{vb}})_{\mathrm{WE}} \quad (8)$$

$$((\mathrm{Ti/Pt–TiO_2}) - \mathrm{e_{cb}})_{\mathrm{WE}} + (\mathrm{O_2})_{\mathrm{s}} \Rightarrow ((\mathrm{Ti/Pt–TiO_2})(\mathrm{O_2^-})_{\mathrm{s}})_{\mathrm{WE}} \quad (9)$$

$$(\mathrm{O_2^-})_{\mathrm{s}} + \text{methyl orange} \Rightarrow \cdots \cdots \Rightarrow \mathrm{CO_2} + \text{inorganic ions} \quad (10)$$

In addition, the recombination between the excited electrons and holes as a reverse reaction of Equation 1 is a significant factor in reducing PEC oxidation efficiency. Therefore, reducing the recombination of electrons and holes is essential to promote PEC efficiency. In this experiment the connection between the working and counter electrodes by the potentiostat made it possible to efficiently drive the photogenerated electrons away from the Ti/$TiO_2$ surface and extend the lifetime of the holes.

## 4. Conclusions

Two novel photoelectrodes of Ti/$TiO_2$ mesh and Ti/Pt–$TiO_2$ mesh were successfully prepared by anodizing Ti mesh in 0.5 M $H_2SO_4$ solutions. The results of XRD analysis indicated that the anatase phase of $TiO_2$ was dominant on the surface of the electrodes, while the results of SEM examination showed that this Ti/$TiO_2$-mesh electrode had a microporous surface structure and its pore size was affected by the anodizing voltage and current density. The XRD results also showed that the intensity of all anatase and rutile peaks increased with the increase in platinum content on the Ti/$TiO_2$ mesh surface. XPS measurements showed that the binding energy of O 1s and Ti 2p increased slightly owing to platinum deposition and that $Pt^0$ as metallic platinum, $Pt^{2+}$ as $Pt(OH)_2$, and $Pt^{4+}$ as either $PtO_2$ or $PtCl_6^{2-}$ presented on the surface of Ti/Pt–$TiO_2$ meshes. The Ti/$TiO_2$ mesh prepared at 160 V and 110 mA $cm^{-2}$ had the best PEC reactivity for methyl orange photooxidation. The PEC reactivity was significantly promoted by applying an electrical bias between the working electrode and counter electrode, since the recombination of electrons and holes was hindered.

## Acknowledgement

The authors thank the Hong Kong Government Research Grant Committee for financial support under the RGC Grant (RGC: PolyU 5030/98E). The authors also thank Mr Michael Campbell for English proofreading.

## References

1. M.R. Hoffmann, S.T. Martin, W. Choi and D.W. Bahnemann, *Chem. Rev.* **95** (1995) 69.
2. A. Linsebigler, G. Lu and J.T. Yates, *Chem. Rev.* **95** (1995) 735.
3. H. Hidaka, T.S. Kazuhiko, J.C. Zhao and N. Serpone, *J. Photochem. Photobiol.* A **109** (1997) 165.
4. A. Fujishima and K. Honda, *Nature* **238** (1972) 37.
5. D.H. Kim and M.A. Anderson, Environ. *Sci. Technol.* **28** (1994) 479.
6. H. Hidaka, T.S. Kazuhiko, J.C. Zhao and N. Serpone, *J. Photochem. Photobiol. A* **64**(1) (1992) 103.
7. K. Vinodgopal, S. Hotchandani and P.V. Kamat, *J. Phys. Chem.* **97** (1993) 9040.
8. X-Z. Li, H-L. Liu, P-T. Yue and Y-P. Sun, *Environ. Sci. Technol.* **34** (2000) 4401.
9. K. Leitner and J.W. Schultze, *J. Electrochem. Soc.* **133** (1986) 1561.